IEEE Access
Multidisciplinary | Rapid Review | Open Access Journal

Received October 27, 2021, accepted November 3, 2021, date of publication November 8, 2021, date of current version November 12, 2021.

Digital Object Identifier 10.1109/ACCESS.2021.3126148

A Novel Weighted Localization Method in Wireless Sensor Networks Based on Hybrid RSS/AoA Measurements

WEIZHONG DING, SHENGMING CHANG, AND JUN LI
School of Electronic and Information Engineering, Ningbo University of Technology, Ningbo 315211, China

Corresponding author: Shengming Chang (csm20130504@163.com)

This work was supported by the Zhejiang Natural Science Foundation under Grant LY18F010020.

ABSTRACT A hybrid RSS/AOA indoor localization method based on error variance and measurement noise weighted least squares (ENWLS) is proposed. This method is based on three-dimensional wireless sensor networks, and achieves high-precision indoor positioning without increasing its complexity. We use the first-order Taylor approximation to approximate the linear weighted least square (WLS) error, and use the weighted least squares estimation to roughly estimate the location of the target, then determine the weight matrix by estimating the linear WLS error variance and the measured noise value on the sensor node. Simulation results show that our proposed method is better than other existing hybrid RSS/AOA localization methods.

INDEX TERMS Wireless sensor networks (WSNs), weighted least square (WLS), received signal strength (RSS), angle of arrival (AOA), localization.

I. INTRODUCTION

In recent years, localization method plays an increasingly important role in wireless sensor networks (WSNs) [1]–[12]. WSNs are wireless networks composed of sensors. In outdoor environment, thanks to GPS and cellular network, mobile terminal location can achieve high accuracy. However, in indoor environment or with serious shadowing effect, satellite and cellular signals are often interrupted, and localization becomes a problem. This paper introduces an indoor localization method based on WSNs. WSNs are composed of anchors which locations are known and targets which locations are unknown. The location of the targets are determined by the location of the anchors and the measurements of radio signals.

Traditional radio signals include time of arrival (TOA) [13]–[17], time difference of arrival (TDOA) [18], [19], angle of arrival (AOA) [20]–[25] and received signal strength (RSS) [26]–[32]. Generally, the localization method based on independent signal has low accuracy. The hybrid localization methods can be combinations of the four radio signals. It is up to the sensor hardware to decide which kind of measurement method to adopt. Usually, one of RSS, TOA and TDOA is combined with AOA, because RSS, TOA and TDOA are distance related measurements, while AOA is angle related measurement. TOA has good localization accuracy, but it requires clock synchronization between anchors and targets. Obviously, realizing this task is highly challenging and will lead to an increase in the cost and the size of mobile devices. TDOA only needs the clock synchronization of anchors. Generally, the locations of anchors are unchanged, so TDOA can usually be wire and wireless. Compared with TOA, the hardware requirements of TDOA are lower, but more anchors are needed to ensure its accuracy. Since the radio signal travels continuously in the air, AOA can be calculated according to the phase difference of the radio signal reaching different antennas. And using antenna arrays is a common method to measure AOA. In the third-generation mobile telecommunication, antenna arrays were widely used in the base stations. Therefore, the base stations can provide AOA measurements at the mobile terminal and we can use it for positioning. Well, RSS measurements can also be obtained through the base stations. RSS and AOA do not require time synchronization, so they have low requirements for hardware, but they also have defects. Due to the multipath effect, the accuracy of RSS and AOA is greatly reduced in complex terrain, so RSS and AoA are more suitable for open terrain. The goal of this paper is to achieve open indoor positioning, so Non Line of Sight (NLOS) is not considered. Using hybrid RSS/AOA measurements can effectively reduce the impact of measurement noises and greatly improve the localiza-

The associate editor coordinating the review of this manuscript and approving it for publication was Prakasam Periasamy.

tion accuracy. Due to the strict requirements of TOA and TDOA for precise timing synchronization in measurement, the cost of the hybrid TOA/AOA measurement and the hybrid TDOA/AOA measurements are greatly increased. Therefore, the hybrid RSS/AOA measurements [33]–[36] provides an attractive low-cost solution for indoor localization problems.

In theory, the estimation of the target node location can be completely accurate according to the exact RSS/AOA measurement. However, due to the RSS/AOA measurement error, the localization problem becomes an NP hard problem. Target position estimation based on hybrid RSS/AOA measurement is an optimization problem of non-convex system, and the challenge is to overcome the noise of the measurement. Semi-definite programming (SDP) and second-order cone programming (SOCP) can effectively solve this problem [37]. The SDP/SOCP method proposed by Chang *et al.* [38] uses the SDP and SOCP methods to transform the non-convex system into a convex system, which has good accuracy. However, the complexity of these methods are too high. The calculation process may delay the positioning. Therefore, it is more practical to use the least square (LS) method to estimate the location after the measurement model is linearized [39]. This method not only has good estimation accuracy, but also greatly reduces the complexity. The weighted least square (WLS) method proposed by Tomic *et al.* [40] improves the accuracy of estimation without increasing the complexity. But the weight that only changes with the distances between target and anchors is not the best. The error covariance WLS (ECWLS) proposed by Kang *et al.* [41] changes the weight. First, they use the LS method to estimate the approximate location of the target, and then calculate the approximate error covariance matrix according to the approximate position. The approximate error covariance matrix is used as the weight. Due to the limitation of the number of anchors, the estimation of the variance of measurement noise has large error. This method directly multiplies the estimated of the variance of the measurement noise into the weight, which will increase the error. The two-step error variance-weighted least squares (TELS) proposed by Watanabe is based on AOA measurement [42]. He uses the LS method to estimate the approximate location of the target, and then calculates the variance as the weight. While he only used AOA measurements, that causes a larger error. The above two methods only consider the influence of the noise variance of evaluation function item, but do not consider the influence of the noise value of the measurements. When the noise standard deviation is the same, the one with small noise value should have more weight.

This paper presents an indoor location method with better performance without increasing the complexity, called error variance and noise value WLS (ENWLS). First, the approximate location of the target is estimated by WLS. Then, according to the theoretical derivation and the approximate location of the target, the variance of each anchor and each evaluation function are calculated. Second, the noise values of the measurements are calculated. Finally, the two items are used as the weight of each anchor and each evaluation function. This method called ''ECWLS''. Its performance is better than the existing methods. The simulation results confirm that. Its complexity is the same as the existing method in linear time. In summary, the main contribution of this paper is to propose a hybrid RSS/AOA target indoor localization method witch performance is best.

The rest of this paper is as follows. The Section II introduces the models of the measurements and the related WLS method. The Section III introduces the establishment of the problem and the proposed ENWLS method. The Section IV gives the simulations, the clarifications on comparisons' figures and the complexity analyzes. The Section V summarizes this paper and introduces the future works of the proposed method.

II. RELATED WORKS

This section describes the model of hybrid RSS/AOA measurement and the overview of three existing weighted localization method with good performance. Their shortcomings are also described.

In the WLS method, the weight that only relates to distance is not the best. In the ECWLS method, due to the limited number of anchors, the estimation of the variance of measurement noise is not accurate. In the TELS method, it is assumed that the variance of measurement noise is the same, the influence of measurement noise on weight is not considered. And the RSS measurements are not used in the TELS method, that reduced the accuracy.

A. SYSTEM MODEL

Consider a wireless sensor networks (WSNs) with N anchors located at $\mathbf{s}_i = [s_{i1}, s_{i2}, s_{i3}]^T \in \mathbb{R}^3$ for i $= 1, \cdots, N$, and $\mathbf{x} = [x_1, x_2, x_3]^T$ is the unknown location of the sensor (target). The distance between the target and the i-th anchor is $\|\mathbf{x} - \mathbf{s}_i\|$, ϕ_i and α_i are true azimuth angles and true elevation angles of AOA, respectively. FIGURE 1 shows the illustration of anchor and target in 3D place. The true values of RSS are given by (1). The true values of AOA are given by (2) and (3)

$$P_i = P_0 - 10\gamma \log_{10} \frac{\|\mathbf{x} - \mathbf{s}_i\|}{d_0}, \quad i = 1, \ldots, N \tag{1}$$

$$\phi_i = \arctan\left(\frac{x_2 - s_{i2}}{x_1 - s_{i1}}\right), \quad i = 1, \ldots, N \tag{2}$$

$$\alpha_i = \arccos\left(\frac{x_3 - s_{i3}}{\|\mathbf{x} - \mathbf{s}_i\|}\right), \quad i = 1, \ldots, N \tag{3}$$

where $\phi_i \in (-\pi, \pi)$ and $\alpha_i \in (-\frac{\pi}{2}, \frac{\pi}{2})$.

In the case of actual measurement error, the measurements of RSS and AoA are given by (4)

$$\hat{P}_i = P_i + n_i \tag{4a}$$

$$\hat{\phi}_i = \phi_i + m_i \tag{4b}$$

$$\hat{\alpha}_i = \alpha_i + v_i \tag{4c}$$

where n_i, m_i, v_i are the measurement errors. The measurement errors in reality are very complicated. We use the noise value

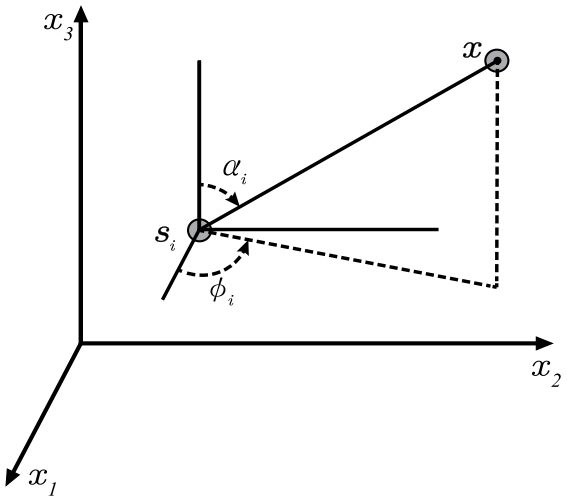

FIGURE 1. Illustration of anchor and target in 3D place.

of positive distribution to simulate the real situations. n_i, m_i, v_i are the independent white zero mean Gaussian noises of received power, azimuth and elevation respectively, and are modeled as $n_i \sim N\left(0, \sigma_{\mathrm{n}_i}^2\right), m_i \sim N\left(0, \sigma_{\mathrm{m}_i}^2\right), v_i \sim N\left(0, \sigma_{\mathrm{v}_i}^2\right)$.

B. WEIGHTED LEAST SQUARES (WLS)

In [40], the WLS method is proposed. By resorting to spherical coordinates, $\|\mathbf{x}-\mathbf{s}_i\|$ was expressed as $\mathbf{u}_i{}^T(\mathbf{x}-\mathbf{s}_i)$ for $i=1,\cdots,N$. For simplicity, the unit vector $\mathbf{u}_i$ was defined by the values of RSS with actual measurement error as

$$\mathbf{u}_i = \left[\cos\hat{\phi}_i \sin\hat{\alpha}_i, \sin\hat{\phi}_i \sin\hat{\alpha}_i, \cos\hat{\alpha}_i\right]^T \tag{5}$$

Equation (4a), (4b) and (4c) can be transformed into

$$\hat{\lambda}_i \mathbf{u}_i{}^T(\mathbf{x}-\mathbf{s}_i) = \eta d_0 + \varepsilon_{1i} \tag{6}$$
$$\mathbf{c}_i{}^T(\mathbf{x}-\mathbf{s}_i) = \varepsilon_{2i} \tag{7}$$
$$\left(\cos\alpha_i \mathbf{u}_i{}^T - \mathbf{k}^T\right)(\mathbf{x}-\mathbf{s}_i) = \varepsilon_{3i} \tag{8}$$

where $\hat{\lambda}_i = 10^{\frac{\hat{P}_i}{10\gamma}}$, $\eta = 10^{\frac{P_0}{10\gamma}}$, $\mathbf{c}_i = [-\sin\phi_i, \cos\phi_i, 0]^T$, $k=[0,0,1]^T$.

WLS is used to estimate the value of $\mathbf{x}$ as

$$\begin{aligned}\hat{\mathbf{x}}_{WLS} = \arg\min_{\mathbf{x}} &\sum_{i=1}^{N}\left(w_i\left(\hat{\lambda}_i \mathbf{u}_i{}^T(\mathbf{x}-\mathbf{s}_i) - \eta d_0\right)\right)^2 \\ &+\sum_{i=1}^{N}\left(w_i\left(\mathbf{c}_i{}^T(\mathbf{x}-\mathbf{s}_i)\right)\right)^2 \\ &+\sum_{i=1}^{N}\left(w_i\left(\cos\alpha_i \mathbf{u}_i{}^T - \mathbf{k}^T\right)(\mathbf{x}-\mathbf{s}_i)\right)^2\end{aligned} \tag{9}$$

The problem (9) can be written in a vector form as

$$\min_{\mathbf{x}} \|\mathbf{W}(\mathbf{A}\mathbf{x}-\mathbf{b})\| \tag{10}$$

where

$$\mathbf{A} = \begin{bmatrix} \vdots \\ \hat{\lambda}_i \mathbf{u}_i{}^T \\ \vdots \\ \mathbf{c}_i{}^T \\ \vdots \\ \cos\alpha_i \mathbf{u}_i{}^T - \mathbf{k}^T \\ \vdots \end{bmatrix} \in \mathbb{R}^{3N\times 3},$$

$$\mathbf{b} = \begin{bmatrix} \vdots \\ \hat{\lambda}_i \mathbf{u}_i{}^T \mathbf{s}_i + \eta d_0 \\ \vdots \\ \mathbf{c}_i{}^T \mathbf{s}_i \\ \vdots \\ \left(\cos\alpha_i \mathbf{u}_i{}^T - \mathbf{k}^T\right)\mathbf{s}_i \\ \vdots \end{bmatrix} \in \mathbb{R}^{3N},$$

$$\mathbf{W} = \mathrm{diag}\left([\mathbf{w},\mathbf{w},\mathbf{w}]\right), \quad w_i = 1 - \frac{\hat{d}_i}{\sum_{i=1}^{N}\hat{d}_i}, \quad \hat{d}_i = d_0 10^{\frac{P_0-\hat{P}_i}{10\gamma}}.$$

The closed-form solution in (10) is (11)

$$\hat{\mathbf{x}}_{WLS} = \left(\mathbf{A}^T\mathbf{W}^T\mathbf{W}\mathbf{A}\right)^{-1}\mathbf{A}^T\mathbf{W}^T\mathbf{W}\mathbf{b} \tag{11}$$

However, the weight that only relates to distance is not the best.

C. ERROR COVARIANCE WLS (ECWLS)

In [41], the ECWLS method is proposed. First, transform the measurement model (4a), (4b), (4c) into (6), (7), (8) respectively. Then the approximate location of the target is roughly calculated by the LS method in [39] as

$$\mathbf{x}_{LS} = \left(\mathbf{A}^T\mathbf{A}\right)^{-1}\mathbf{A}^T\mathbf{b} \tag{12}$$

ε_{1i}, ε_{2i} and ε_{3i} in (6), (7), (8) can be expressed as

$$\begin{aligned}\varepsilon_{1i} = &\hat{\lambda}_i \cos\hat{\phi}_i \sin\hat{\alpha}_i (x_1 - s_{i1}) \\ &+\hat{\lambda}_i \sin\hat{\phi}_i \sin\hat{\alpha}_i (x_2 - s_{i2}) \\ &+\hat{\lambda}_i \cos^2\hat{\alpha}_i (x_3 - s_{i3}) - \eta d_0\end{aligned} \tag{13a}$$
$$\varepsilon_{2i} = -\sin\hat{\phi}_i (x_1 - s_{i1}) + \cos\hat{\phi}_i (x_2 - s_{i2}) \tag{13b}$$
$$\begin{aligned}\varepsilon_{3i} = &\frac{1}{2}\sin 2\hat{\alpha}_i \cos\hat{\phi}_i (x_1 - s_{i1}) \\ &+\frac{1}{2}\sin 2\hat{\alpha}_i \sin\hat{\phi}_i (x_2 - s_{i2}) \\ &+\sin^2\hat{\alpha}_i (x_3 - s_{i3})\end{aligned} \tag{13c}$$

Assuming that the measurement noises are small enough, $\hat{\lambda}_i$, $\sin\hat{\phi}_i$ and $cos\hat{\alpha}_i$ are expanded by second-order Taylor expansion as follows,

$$\begin{aligned}\hat{\lambda}_i &= 10^{\frac{P_i+n_i}{10\gamma}} = \lambda_i 10^{\frac{n_i}{10\gamma}} \\ &\approx \lambda_i\left(1 + \overline{\gamma} n_i + \frac{1}{2}\overline{\gamma}^2 n_i^2\right)\end{aligned} \tag{14a}$$

$$\sin\hat{\phi}_i = \sin(\phi_i + m_i) \approx \sin\phi_i + \cos(\phi_i)\, m_i - \frac{1}{2}\sin(\phi_i)\, m_i^2 \quad (14b)$$

$$\cos\hat{\alpha}_i = \cos\left(\hat{\alpha}_i + v_i\right) \approx \cos\alpha_i - \sin(\alpha_i)\, v_i - \frac{1}{2}\cos(\alpha_i)\, v_i^2 \quad (14c)$$

where $\overline{\gamma} = \frac{\ln 10}{10\gamma}$.

Using $\mathbf{x}_{LS}$ instead of $\mathbf{x}$ and substitute (14) for (13), get the estimates of ε_{1i}, ε_{2i} and ε_{3i} as

$$\begin{aligned}\hat{\varepsilon}_{1i} = {} & \eta d_0 \overline{\gamma} n_i + \lambda_i \left(r_i \cos\alpha_i - \sin(\alpha_i)\, d_{i3}\right) v_i \\ & + \frac{1}{2}\eta d_0 \overline{\gamma}^2 {n_i}^2 - \frac{1}{2}\lambda_i r_i \sin(\alpha_i)\, {m_i}^2 \\ & - \frac{1}{2}\lambda_i \left(r_i \sin\hat{\alpha}_i + \cos(\alpha_i)\, d_{i3}\right) v_i^2 \end{aligned} \quad (15a)$$

$$\hat{\varepsilon}_{2i} = -r_i m_i \quad (15b)$$

$$\begin{aligned}\hat{\varepsilon}_{3i} = {} & \left(\cos(2\alpha_i)\, r_i - \sin(2\alpha_i)\, d_{i3}\right) v_i \\ & - \frac{1}{4}\sin(2\alpha_i)\, r_i m_i^2 - \left(\sin(2\alpha_i)\, r_i - \cos(2\alpha_i)\, d_{i3}\right) v_i^2 \\ & + \frac{1}{2}\sin(2\alpha_i)\, r_i - \sin^2(2\alpha_i)\, d_{i3} \end{aligned} \quad (15c)$$

where $r_i = \sqrt{(x_{LS1} - s_{i1})^2 + (x_{LS2} - s_{i2})^2}$, $d_{i3} = x_{LS3} - s_{i3}$, $\lambda_i = 10^{\frac{\hat{P}_i}{10\gamma}} = 10^{\frac{P_0 - 10\gamma\log_{10}\frac{\|\mathbf{x}_{LS} - \mathbf{s}_i\|}{d_0}}{10\gamma}}$. The value of P_i, ϕ_i and α_i are estimated by $\mathbf{x}_{LS}$ as $\overline{P}_i$, $\overline{\phi}_i$ and $\overline{\alpha}_i$ as follows,

$$\overline{P}_i = P_0 - 10\gamma\log_{10}\frac{\|\mathbf{x}_{LS} - \mathbf{s}_i\|}{d_0} \quad (16a)$$

$$\overline{\phi}_i = \tan^{-1}\left(\frac{x_{LS2} - s_{i2}}{x_{LS1} - s_{i1}}\right) \quad (16b)$$

$$\overline{\alpha}_i = \cos^{-1}\left(\frac{x_{LS3} - s_{i3}}{\|\mathbf{x}_{LS} - \mathbf{s}_i\|}\right) \quad \text{for} \quad i = 1, \cdots, N. \quad (16c)$$

Calculation of $\hat{\sigma}_{n_i}$, $\hat{\sigma}_{m_i}$, $\hat{\sigma}_{v_i}$

$$\hat{\sigma}_{n_i}^2 = \frac{1}{N}\sum_{i=1}^{N}\left(\hat{P}_i - \overline{P}_i\right)^2 \quad (17a)$$

$$\hat{\sigma}_{m_i}^2 = \frac{1}{N}\sum_{i=1}^{N}\left(\hat{\phi}_i - \overline{\phi}_i\right)^2 \quad (17b)$$

$$\hat{\sigma}_{v_i}^2 = \frac{1}{N}\sum_{i=1}^{N}\left(\hat{\alpha}_i - \overline{\alpha}_i\right)^2 \quad (17c)$$

The covariance matrix is composed of the variances and covariances of $\hat{\varepsilon}_{1i}$, $\hat{\varepsilon}_{2i}$ and $\hat{\varepsilon}_{3i}$. The variances and covariances of $\hat{\varepsilon}_{1i}$, $\hat{\varepsilon}_{2i}$ and $\hat{\varepsilon}_{3i}$ are as

$$\begin{aligned}\mathrm{Var}\left(\hat{\varepsilon}_{1i}\right) = {} & E\left(\left(\hat{\varepsilon}_{1i} - E\left[\hat{\varepsilon}_{1i}\right]\right)^2\right) \\ = {} & (\eta d_0 \overline{\gamma})^2 \hat{\sigma}_{n_i}^2 + \left(\lambda_i \left(r_i \cos\alpha_i - \sin(\alpha_i)\, d_{i3}\right)\right)^2 \hat{\sigma}_{v_i}^2 \\ & + \frac{1}{2}\left(\eta d_0 \overline{\gamma}^2\right)^2 \hat{\sigma}_{n_i}^4 + \frac{1}{2}\left(\lambda_i r_i \sin(\alpha_i)\right)^2 \hat{\sigma}_{m_i}^4 \\ & + \frac{1}{2}\left(\lambda_i \left(r_i \sin\hat{\alpha}_i + \cos(\alpha_i)\, d_{i3}\right)\right)^2 \hat{\sigma}_{v_i}^4 \end{aligned} \quad (18a)$$

$$\mathrm{Var}\left(\hat{\varepsilon}_{2i}\right) = E\left(\left(\hat{\varepsilon}_{2i} - E\left[\hat{\varepsilon}_{2i}\right]\right)^2\right) = r_i^2 \hat{\sigma}_{m_i}^2 \quad (18b)$$

$$\begin{aligned}\mathrm{Var}\left(\hat{\varepsilon}_{3i}\right) = {} & E\left(\left(\hat{\varepsilon}_{3i} - E\left[\hat{\varepsilon}_{3i}\right]\right)^2\right) \\ = {} & \left(\cos(2\alpha_i)\, r_i - \sin(2\alpha_i)\, d_{i3}\right)^2 \hat{\sigma}_{v_i}^2 \\ & + \frac{1}{8}\left(\sin(2\alpha_i)\, r_i\right)^2 \hat{\sigma}_{m_i}^4 \\ & + 2\left(\sin(2\alpha_i)\, r_i - \cos(2\alpha_i)\, d_{i3}\right)^2 \hat{\sigma}_{v_i}^4 \end{aligned} \quad (18c)$$

$$\begin{aligned}\mathrm{Cov}\left(\hat{\varepsilon}_{1i}, \hat{\varepsilon}_{3i}\right) = {} & E\left(\left(\hat{\varepsilon}_{1i} - E\left[\hat{\varepsilon}_{1i}\right]\right)\left(\hat{\varepsilon}_{3i} - E\left[\hat{\varepsilon}_{3i}\right]\right)\right) \\ = {} & \left(\lambda_i \left(r_i \cos\alpha_i - \sin(\alpha_i)\, d_{i3}\right)\right) \\ & \left(\cos(2\alpha_i)\, r_i - \sin(2\alpha_i)\, d_{i3}\right) \hat{\sigma}_{v_i}^2 \\ & + \frac{1}{4}\lambda_i {r_i}^2 \sin(\alpha_i)\sin(2\alpha_i)\, \hat{\sigma}_{m_i}^4 \\ & + \lambda_i \left(r_i \sin\hat{\alpha}_i + \cos(\alpha_i)\, d_{i3}\right) \\ & \left(\sin(2\alpha_i)\, r_i - \cos(2\alpha_i)\, d_{i3}\right) \hat{\sigma}_{v_i}^4 \end{aligned} \quad (18d)$$

The specific calculation of $\overline{\mathbf{C}}$ is as

$$\overline{\mathbf{C}} = \begin{pmatrix} \mathbf{D}_{11} & \mathbf{0} & \mathbf{D}_{13} \\ \mathbf{0} & \mathbf{D}_{22} & \mathbf{0} \\ \mathbf{D}_{31} & \mathbf{0} & \mathbf{D}_{33} \end{pmatrix} \quad (19)$$

where $\mathbf{D}_{11}$, $\mathbf{D}_{22}$, $\mathbf{D}_{33}$, $\mathbf{D}_{13}$, $\mathbf{D}_{31}$ are diagonal matrices, $\mathbf{D}_{11} = \mathrm{diag}\left(\mathrm{Var}\left(\hat{\varepsilon}_{1i}\right)\right)$, $\mathbf{D}_{22} = \mathrm{diag}\left(\mathrm{Var}\left(\hat{\varepsilon}_{2i}\right)\right)$, $\mathbf{D}_{33} = \mathrm{diag}\left(\mathrm{Var}\left(\hat{\varepsilon}_{3i}\right)\right)$, $\mathbf{D}_{13} = \mathbf{D}_{31} = \mathrm{diag}\left(\mathrm{Cov}\left(\hat{\varepsilon}_{1i}, \hat{\varepsilon}_{3i}\right)\right)$. Then, the covariance matrix of these error terms are used as the weight to calculate the final estimate as

$$\mathbf{x}_{ECWLS} = \left(\mathbf{A}^T \overline{\mathbf{C}}^{-1} \mathbf{A}\right)^{-1} \mathbf{A}^T \overline{\mathbf{C}}^{-1} \mathbf{b} \quad (20)$$

However, due to the limited number of anchors, the estimation of the variance of measurement noise is not accurate. This causes a large error.

D. TWO-STEP ERROR VARIANCE-WEIGHTED LEAST SQUARES (TELS)

In [42], the TELS method is proposed. Unlike WLS and ECWLS, TELS only uses AOA measurements for localization. The closed form solution of the target is obtained by the LS method as

$$\tilde{\mathbf{x}}_{LS} = \left(\tilde{\mathbf{A}}^T \tilde{\mathbf{A}}\right)^{-1} \tilde{\mathbf{A}}^T \tilde{\mathbf{b}} \quad (21)$$

where

$$\widetilde{\mathbf{A}} = \begin{bmatrix} \vdots \\ \mathbf{c}_i^T \\ \vdots \\ \cos\alpha_i \mathbf{u}_i^T - \mathbf{k}^T \\ \vdots \end{bmatrix} \in \mathbb{R}^{2N \times 3},$$

$$\widetilde{\mathbf{b}} = \begin{bmatrix} \vdots \\ \mathbf{c}_i^T \mathbf{s}_i \\ \vdots \\ \left(\cos\alpha_i \mathbf{u}_i^T - \mathbf{k}^T\right) \mathbf{s}_i \\ \vdots \end{bmatrix} \in \mathbb{R}^{2N}.$$

By using the geometric relationship of trigonometric functions, ε_{2i}, ε_{3i} in (4) can be transformed into (22)

$$\begin{aligned}\varepsilon_{2i} &= -(x_1 - s_{i1})\sin\hat{\phi}_i + (x_2 - s_{i2})\cos\hat{\phi}_i \\ &\approx -r_i m_i \qquad (22a)\\ \varepsilon_{3i} &= (x_1 - s_{i1})\cos\hat{\phi}_i\cos\hat{\alpha}_i \\ &\quad + (x_2 - s_{i2})\sin\hat{\phi}_i\cos\hat{\alpha}_i \\ &\quad - (x_3 - s_{i3})\sin\hat{\alpha}_i \approx -d_i v_i \qquad (22b)\end{aligned}$$

where $d_i = \left\|\tilde{\mathbf{x}}_{LS} - \mathbf{s}_i\right\|$. Define that the estimations of ε_{2i} and ε_{3i} are $\hat{\varepsilon}_{2i} = -r_i m_i$ and $\hat{\varepsilon}_{3i} = -d_i v_i$.

The variances of $\hat{\varepsilon}_{2i}$ and $\hat{\varepsilon}_{3i}$ are calculated as

$$\mathrm{Var}\left(\hat{\varepsilon}_{2i}\right) = E\left(\left(\hat{\varepsilon}_{2i} - E\left[\hat{\varepsilon}_{2i}\right]\right)^2\right) = r_i^2\sigma_{m_i}^2 \qquad (23a)$$

$$\mathrm{Var}\left(\hat{\varepsilon}_{3i}\right) = E\left(\left(\hat{\varepsilon}_{3i} - E\left[\hat{\varepsilon}_{3i}\right]\right)^2\right) = d_i^2\sigma_{v_i}^2 \qquad (23b)$$

Assuming that $\sigma_{m_i} = \sigma_{v_i}$. Replace σ_{m_i} and σ_{v_i} with σ. Then, (23) can be written as

$$\mathrm{Var}\left(\hat{\varepsilon}_{2i}\right) = r_i^2\sigma^2 \qquad (24a)$$

$$\mathrm{Var}\left(\hat{\varepsilon}_{3i}\right) = d_i^2\sigma^2 \qquad (24b)$$

The weight matrix relates to (24) as

$$\tilde{w}_{1i} = \frac{\sigma^2}{\mathrm{Var}\left(\hat{\varepsilon}_{2i}\right)} \qquad (25a)$$

$$\tilde{w}_{2i} = \frac{\sigma^2}{\mathrm{Var}\left(\hat{\varepsilon}_{3i}\right)} \qquad (25b)$$

Then, these error terms is used as the weight to calculate the final estimate as

$$\mathbf{x}_{TELS} = \left(\tilde{\mathbf{A}}^T\tilde{\mathbf{W}}^{-1}\tilde{\mathbf{A}}\right)^{-1}\tilde{\mathbf{A}}^T\tilde{\mathbf{W}}^{-1}\tilde{\mathbf{b}} \qquad (26)$$

The advantage of the TELS method is that, it doesn't need previous environmental information. Although environmental information is uncertain, it always changes in a certain range. RSS measurements are very easy to get. Therefore, the measurement accuracy will be reduced if the RSS measurements are not used. And the influence of measurement noise on weight is not considered in this method.

In order to improve the accuracy, we add the RSS measurements into the method with appropriate weight, which is related to error variance and the measured noise value on the sensor nodes.

III. PROBLEM FORMULATION AND THE PROPOSED METHOD

This section gives the ML estimate which is difficult to solve and the ENWLS method is described. First, calculate the approximate value of $\mathbf{x}_{WLS}$ with the WLS method. Then calculate weight matrix $\mathbf{C}$ and $\mathbf{S}$ with $\mathbf{x}_{WLS}$. Finally, calculate the approximate value of $\mathbf{x}_{ENWLS}$, with the weight, $\mathbf{CS}$. FIGURE 2 shows a flowchart of the proposed method and the symbol expression and definition of the main variables in this section are listed in Table 1.

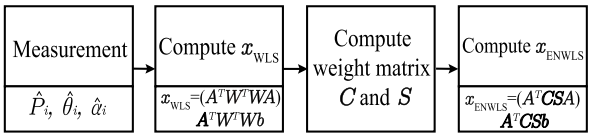

FIGURE 2. The flowchart of the ENWLS method.

TABLE 1. The symbol and definition of main variables.

Symbol	Definition
$\hat{P}_i$	The RSS measurements
$\hat{\phi}_i$	The azimuth angles in the AOA measurements
$\hat{\sigma}_i$	The elevation angles in the AOA measurements
γ	The pass-loss exponent
$\mathbf{x}$	The position of the target
$\mathbf{s}$	The position of the anchors
ε_{1i}	The error of the function item in (28)
ε_{2i}	The error of the function item in (29)
ε_{3i}	The error of the function item in (30)
n_i	The noise of RSS measurements
m_i	The noise of the azimuth angles in the AOA measurements
v_i	The noise of the elevation angles in the AOA measurements
$\mathbf{C}$	The weight matrix related to the variances of ε_{1i}, ε_{2i} and ε_{3i}
$\mathbf{S}$	The weight matrix related to n_i, m_i and v_i

A. PROBLEM FORMULATION

Based on the Gaussian noise measurement models (1), (2), (3) and (4), we can formulate the ML estimator of target location $\mathbf{x}$ as follows,

$$\begin{aligned}\min_{\mathbf{x}} &\sum_{i=1}^{N}\frac{1}{\sigma_{n_i}^2}\left(\hat{P}_i - P_0 + 10\gamma\log_{10}\frac{\|\mathbf{x}-\mathbf{s}_i\|}{d_0}\right)^2 \\ &+\sum_{i=1}^{N}\frac{1}{\sigma_{m_i}^2}\left(\hat{\phi}_i - \arctan(\frac{x_2 - s_{i2}}{x_1 - s_{i1}})\right)^2 \\ &+\sum_{i=1}^{N}\frac{1}{\sigma_{v_i}^2}\left(\hat{\alpha}_i - \arccos(\frac{x_3 - s_{i3}}{\|\mathbf{x}-\mathbf{s}_i\|})\right)^2 \qquad (27)\end{aligned}$$

However, this problem is non-convex and difficult to solve.

B. COMPUTATION OF WEIGHT MATRIX C

The weight matrix $\mathbf{C}$ is related to the variances of each anchor and each evaluation function item. Assuming that $|n_i|$, $|m_i|$ and $|v_i| \ll 1$. Using a first-order Taylor approximation, ε_{1i}, ε_{2i}, ε_{3i} in (6), (7), (8) are written as (28), (29), (30)

$$\varepsilon_{1i} = \eta d_0\frac{\ln 10}{10\gamma}n_i \qquad (28)$$

$$\varepsilon_{2i} = -\left(\cos\hat{\phi}_i(x_1 - s_{i1}) + \sin\hat{\phi}_i(x_2 - s_{i2})\right)m_i \qquad (29)$$

$$\varepsilon_{3i} = \|\mathbf{x} - \mathbf{s}_i\|\sin\hat{\alpha}_i v_i \qquad (30)$$

The variances of (28), (29), (30) are calculated as

$$V(\varepsilon_{1i}) = \left(\eta d_0\frac{\ln 10}{10\gamma}\right)^2\sigma_{n_i}^2 \qquad (31a)$$

$$V(\varepsilon_{2i}) = \left(\cos\hat{\phi}_i(x_1 - s_{i1}) + \sin\hat{\phi}_i(x_2 - s_{i2})\right)^2\sigma_{m_i}^2 \qquad (31b)$$

$$V(\varepsilon_{3i}) = \left(\|\mathbf{x} - \mathbf{s}_i\|\sin\hat{\alpha}_i\right)^2\sigma_{v_i}^2 \qquad (31c)$$

Due to the limited number of anchor nodes, the estimations of σ_{n_i}, σ_{m_i}, σ_{v_i} are not accurate. So, assume that $\sigma_{n_i} = \sigma_{m_i} =$

$\sigma_{v_i} = \sigma$. The influence of different standard deviation and noise value of each anchor and each evaluation function item will be reflected in weight matrix $\mathbf{S}$. (31) can be written in a equivalent form as

$$V(\varepsilon_{1i}) = \left(\eta d_0 \frac{\ln 10}{10\gamma}\right)^2 \sigma^2 \tag{32a}$$

$$V(\varepsilon_{2i}) = \left(\cos\hat{\phi}_i (x_1 - s_{i1}) + \sin\hat{\phi}_i (x_2 - s_{i2})\right)^2 \sigma^2 \tag{32b}$$

$$V(\varepsilon_{3i}) = \left(\|\mathbf{x} - \mathbf{s}_i\| \sin\hat{\alpha}_i\right)^2 \sigma^2 \tag{32c}$$

The weights of each anchor and each evaluation function item are inversely proportional to their variance, so the weight matrix $\mathbf{C}$ can be written as

$$C_{1i} = \frac{1}{V(\varepsilon_{1i})} \tag{33a}$$

$$C_{2i} = \frac{1}{V(\varepsilon_{2i})} \tag{33b}$$

$$C_{3i} = \frac{1}{V(\varepsilon_{3i})} \quad \text{for} \quad i = 1, \cdots, N \tag{33c}$$

It does not affect the final estimate that multiply each term of the weights in $\mathbf{C}$ by σ^2. Replace $\mathbf{x}$ with the estimate of $\mathbf{x}$, $\hat{\mathbf{x}}_{WLS}$. So, (33) can be written as

$$C_{1i} = \frac{\sigma^2}{V(\varepsilon_{1i})} = \frac{1}{\left(\eta d_0 \frac{\ln 10}{10\gamma}\right)^2} \tag{34a}$$

$$C_{2i} = \frac{\sigma^2}{V(\varepsilon_{2i})} = \frac{1}{\left(\cos\hat{\phi}_i \left(\hat{x}_{WLS1} - s_{i1}\right) + \sin\hat{\phi}_i \left(\hat{x}_{WLS2} - s_{i2}\right)\right)^2} \tag{34b}$$

$$C_{3i} = \frac{\sigma^2}{V(\varepsilon_{3i})} = \frac{1}{\left(\|\hat{\mathbf{x}}_{WLS} - \mathbf{s}_i\| \sin\hat{\alpha}_i\right)^2} \quad \text{for} \quad i = 1, \cdots, N \tag{34c}$$

The matrix $\mathbf{C}$ consists of $\mathbf{C}_1$, $\mathbf{C}_2$ and $\mathbf{C}_3$

$$\mathbf{C} = \text{diag}(\mathbf{C}_1, \mathbf{C}_2, \mathbf{C}_3) \tag{35}$$

C. COMPUTATION OF WEIGHT MATRIX S

The weight matrix $\mathbf{S}$ is related to the values of n_i, m_i and v_i. n_i, m_i and v_i can be estimated by $\hat{\mathbf{x}}_{WLS}$ as

$$\hat{n}_i = \hat{P}_i - P_0 + 10\gamma \log_{10} \frac{\|\hat{\mathbf{x}}_{WLS} - \mathbf{s}_i\|}{d_0} \tag{36a}$$

$$\hat{m}_i = \hat{\phi}_i - \arctan\left(\frac{\hat{x}_{WLS2} - s_{i2}}{\hat{x}_{WLS1} - s_{i1}}\right) \tag{36b}$$

$$\hat{v}_i = \hat{\alpha}_i - \arccos\left(\frac{\hat{x}_{WLS3} - \mathrm{s}_{i3}}{\|\hat{\mathbf{x}}_{WLS} - \mathbf{s}_i\|}\right) \quad \text{for} \quad i = 1, \cdots, N \tag{36c}$$

The weight matrix $\mathbf{S}$ can be written as (37) and (38)

$$S_{1i} = 1 - \frac{|\hat{n}_i|}{\sum_{i=1}^{N} |\hat{n}_i| + \sum_{i=1}^{N} |\hat{m}_i| + \sum_{i=1}^{N} |\hat{v}_i|} \tag{37a}$$

$$S_{2i} = 1 - \frac{|\hat{m}_i|}{\sum_{i=1}^{N} |\hat{n}_i| + \sum_{i=1}^{N} |\hat{m}_i| + \sum_{i=1}^{N} |\hat{v}_i|} \tag{37b}$$

$$S_{3i} = 1 - \frac{|\hat{v}_i|}{\sum_{i=1}^{N} |\hat{n}_i| + \sum_{i=1}^{N} |\hat{m}_i| + \sum_{i=1}^{N} |\hat{v}_i|} \quad \text{for} \quad i = 1, \cdots, N \tag{37c}$$

The matrix $\mathbf{S}$ consists of $\mathbf{S}_1$, $\mathbf{S}_2$ and $\mathbf{S}_3$

$$\mathbf{S} = \text{diag}(\mathbf{S}_1, \mathbf{S}_2, \mathbf{S}_3) \tag{38}$$

D. THE ENWLS ESTIMATE

First, calculate the approximate value of $\mathbf{x}$ with the WLS method in (11).

Then, calculate weight matrix $\mathbf{C}$ and $\mathbf{S}$ with $\hat{\mathbf{x}}_{WLS}$. The ENWLS estimator for the target location, $\mathbf{x}_{ENWLS}$, is derived as follows

$$\begin{aligned}\mathbf{x}_{ENWLS} = \underset{x}{\text{argmin}} &\sum_{i=1}^{N} C_{1i} S_{1i} \left(\lambda_i \mathbf{u}_i{}^T (\mathbf{x} - \mathbf{s}_i) - \eta d_0\right)^2 \\ &+ \sum_{i=1}^{N} C_{2i} S_{2i} \left(\mathbf{c}_i{}^T (\mathbf{x} - \mathbf{s}_i)\right)^2 \\ &+ \sum_{i=1}^{N} C_{3i} S_{3i} \left(\left(\cos\alpha_i \mathbf{u}_i{}^T - \mathbf{k}^T\right)(\mathbf{x} - \mathbf{s}_i)\right)^2\end{aligned} \tag{39}$$

By expressing (39) in matrix form, the estimated target position becomes a closed-form solution as

$$\hat{\mathbf{x}}_{ENWLS} = \left(\mathbf{A}^T \mathbf{C} \mathbf{S} \mathbf{A}\right)^{-1} \mathbf{A}^T \mathbf{C} \mathbf{S} \mathbf{b} \tag{40}$$

IV. ANALYSIS OF RESULTS

In this section, we verify the performance of the proposed method via computer simulations. All observations are generated by using (4). The target and anchors are randomly deployed inside a box with an edge length $B = 15\,\text{m}$ for each Monte Carlo run (M_c). As considered in most existing projects, the reference distance is set to $d_0 = 1\,\text{m}$, the reference path loss to $P_0 = -10\,\text{dBm}$. The PLE changes according to the environmental conditions, so perfect knowledge of the PLE is virtually impossible to obtain in practice. Here, we assume that PLE is a random value in interval [2.2, 2.8] for each Monte Carlo run. Performance is evaluated by calculating the root mean square error (RMSE), defined as $\text{RMSE} = \sqrt{\frac{1}{M_c}\sum_{i=1}^{M_c} \|x_i - \hat{x}_i\|^2}$, where M_c is the Number of runs, x_i is the true location of target in the i-th run, $\hat{x}_i$ is the estimated location of target in the i-th run. M_c is set to 50000. Obviously, the lower RMSE, the better performance.

TABLE 2. Variables of FIGURE 3 to 7.

	σ_{n_i}(dBm)	σ_{m_i}(deg)	σ_{v_i}(deg)	N
FIGURE.3	6	10	1 to 10	10
FIGURE.4	6	1 to 10	10	10
FIGURE.5	1 to 10	10	10	10
FIGURE.6	6	10	10	3 to 11
FIGURE.7	2	4	4	3 to 11

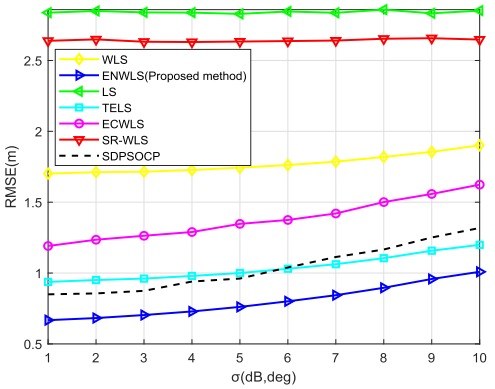

FIGURE 3. RMSE versus standard deviation of elevation angle noise, σ_{v_i}.

The variables of FIGURE 3 to 7 are given in TABLE.1, where σ_{n_i} represents the standard deviation of received power noise, σ_{m_i} represents the standard deviation of azimuth angle noise, σ_{v_i} represents the standard deviation of elevation angle noise, N represents the number of anchor nodes. We compare the performance of our method with the SR-WLS method in [9], the LS method in [39], the WLS method in [40], the ECWLS method in [41], the TELS method in [42] and the SDP/SOCP method in [38].

A. DIFFERENT STANDARD DEVIATIONS OF AZIMUTH ANGLE, ELEVATION ANGLE AND RECEIVED POWER

FIGURE 3 shows the relationship between RMSE and the standard deviation of elevation angle noise, σ_{v_i}. Set the standard deviation of azimuth angle noise σ_{m_i} to 10 deg, the standard deviation of received power noise σ_{n_i} to 6 dBm and the numbers of anchors N to 10. As shown in FIGURE 3, RMSE of all considered methods increases with the increase of σ_{v_i}. The weight matrix $\mathbf{C}$ of the proposed method ENWLS considers the influence of the different noise values of the different measurements. Due to the rationality of the weight of the proposed method, it is the best among all considered methods.

FIGURE 4 shows the relationship between RMSE and the standard deviation of azimuth noise, σ_{m_i}. Set the standard deviation of azimuth angle noise σ_{v_i} to 10 deg, the standard deviation of received power noise σ_{n_i} to 6 dBm and the numbers of anchors N to 10. As shown in FIGURE 4, since the weight of the proposed method relates to the noise values, its performance is better than that of the others.

FIGURE 5 shows the relationship between RMSE and the standard deviation of RSS noise, σ_{n_i}. Set the standard deviation of azimuth angle noise σ_{m_i} to 10 deg, the standard deviation of received power noise σ_{v_i} to 10 deg and the numbers of anchors N to 10. As shown in FIGURE 5, RMSE of the LS method and the SR-WLS method increase rapidly

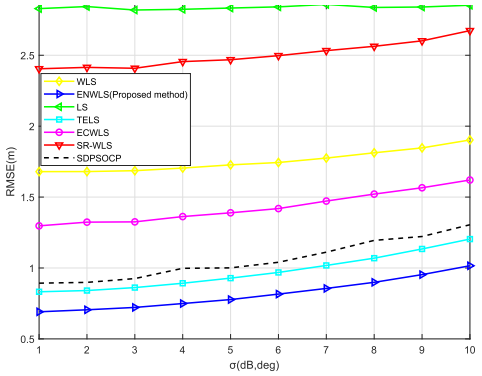

FIGURE 4. RMSE versus standard deviation of azimuth angle noise, σ_{m_i}.

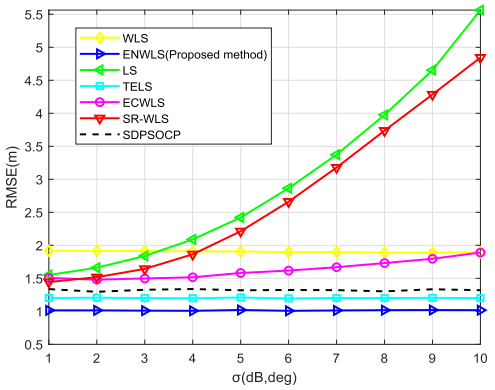

FIGURE 5. RMSE versus standard deviation of received power noise, σ_{n_i}.

with the increase of σ_{n_i}. This is because the weight of RSS measurement is too large. Due to the weight matrix $\mathbf{S}$, the RMSE of the proposed method does not increase significantly with the increase of σ_{n_i}. That is because when σ_{n_i} rises, the weight matrix $\mathbf{S}$ will reduce the weight of the function term corresponding to σ_{n_i} to avoid larger error. This is also the reason why the WLS method and the TELS method are also relatively stable. The proposed method is stable and more accurate.

B. DIFFERENT NUMBERS OF ANCHORS

FIGURE 6 shows the relationship between RMSE and the number of anchors, N, when the measured standard deviation is large. Set the standard deviation of azimuth angle noise σ_{m_i} to 10 deg, the standard deviation of elevation angle noise σ_{v_i} to 10 deg, the standard deviation of received power noise σ_{n_i} to 6 dBm. As shown in FIGURE 6, when the measured standard deviation is large, the RMSE of the proposed method is the best among all methods except when $N = 3$. When $N = 3$, the RMSE of the WLS method is a little better than the proposed method. That is because the number of anchor nodes is too small, resulting in inaccurate estimation of noise value, so there is a large error in the weight matrix $\mathbf{S}$ of the proposed method ENWLS. That causes a negative impact on the RMSE. This is also the reason why the ECWLS method has the worst performance when $N = 3$. However, in practice, the number of anchor nodes is generally more than 3, so the proposed method still has the best performance in practice.

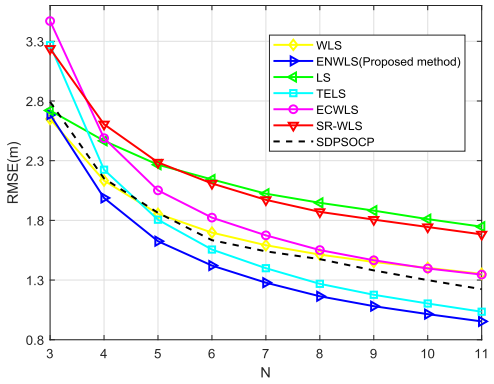

FIGURE 6. RMSE versus *N*, when the measured standard deviation is large.

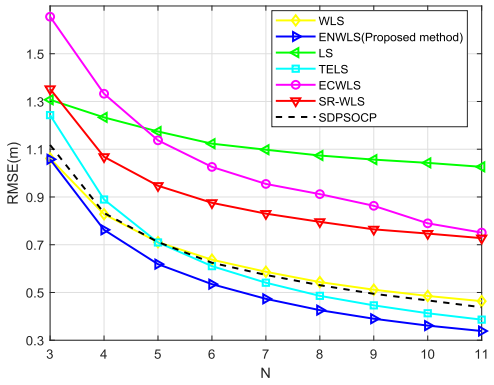

FIGURE 7. RMSE versus *N*, when the measured standard deviation is small.

TABLE 3. Complexity.

Method	Describe	Complexity
SR-WLS	The "SR-WLS" method in [9].	$\mathcal{O}(KN)$
LS	The "LS" method in [39].	$\mathcal{O}(N)$
WLS	The "WLS" method in [40].	$\mathcal{O}(N)$
ECWLS	The "ECWLS" method in [41].	$\mathcal{O}(N)$
TELS	The "TELS" method in [42].	$\mathcal{O}(N)$
SDP/SOCP	The "SDP/SOCP" method in [38].	$\mathcal{O}(N^{3.5})$
ENWLS	The proposed "ENWLS" method.	$\mathcal{O}(N)$

FIGURE 7 shows the relationship between RMSE and the number of anchors, N, when the measured standard deviation is small. Set the standard deviation of azimuth angle noise σ_{m_i} to 4 deg, the standard deviation of elevation angle noise σ_{v_i} to 4 deg, the standard deviation of received power noise σ_{n_i} to 2dBm. Due to the rational use of RSS data, the performance of ENWLS is better than that of TELS. As shown in FIGURE 7, when the measured standard deviation is small, the RMSE of the proposed method is the best among all considered methods.

C. COMPLEXITY ANALYSIS

TABLE.3 shows the complexity of the six methods. Because using WLS to calculate the approximate location of the target localization only requires $\mathcal{O}(N)$, then replace $\mathbf{W}$ with $\mathbf{CS}$ and use WLS again only requires $\mathcal{O}(N)$. Therefore, as with the WLS methods, the calculation amount of this method is $\mathcal{O}(N)$. The complexity of this method is low enough for real-time applications.

However, the complexity of the SR-WLS method and the SDP/SOCP method are $\mathcal{O}(KN)$ and $\mathcal{O}(N^{3.5})$, respectively. Due to using SDP and SOCP methods, the complexity of the SDP/SOCP method is the highest, which may delay the positioning.

V. CONCLUSION

This paper proposes an indoor target localization method, ENWLS, based on hybrid RSS/AOA measurement in 3D wireless sensor networks. This method uses the approximate WLS method, its weight matrix is related to error variance and measurement noise. Its complexity is the same as the existing method in linear time. Simulation results show that this method has better performance than the existing hybrid RSS/AOA position method.

As the future work on this method, the system model will be considered closer to the actual situation. We will consider multi-user situation. Users can also receive RSS measurements from each other, which will make the positioning more accurate. Multipath effect will be considered. We will try to reduce the impact of multipath effect through rigorous mathematical derivation. In the actual situation, the interior structure may be complicated. Therefore, we will add the impact of NOLS, so that our method can be applied in more actual scenarios.

REFERENCES

[1] S. Bartoletti, W. Dai, A. Conti, and M. Z. Win, "A mathematical model for wideband ranging," *IEEE J. Sel. Topics Signal Process.*, vol. 9, no. 2, pp. 216–228, Mar. 2015, doi: 10.1109/JSTSP.2014.2370934.

[2] R. Goyat, G. Kumar, M. Alazab, R. Saha, R. Thomas, and M. K. Rai, "A secure localization scheme based on trust assessment for WSNs using blockchain technology," *Future Gener. Comput. Syst.*, vol. 125, pp. 221–231, Dec. 2021, doi: 10.1016/j.future.2021.06.039.

[3] S. Tomic, M. Beko, and R. Dinis, "Distributed RSS-AoA based localization with unknown transmit powers," *IEEE Wireless Commun. Lett.*, vol. 5, no. 4, pp. 392–395, Aug. 2016, doi: 10.1109/LWC.2016.2567394.

[4] J. Liu, L. Sun, J. Pu, and Y. Yan, "Hybrid cooperative localization based on robot-sensor networks," *Signal Process.*, vol. 188, Nov. 2021, Art. no. 108242, doi: 10.1016/j.sigpro.2021.108242.

[5] K. Shah and D. Jinwala, "Privacy preserving secure expansive aggregation with malicious node identification in linear wireless sensor networks," *Frontiers Comput. Sci.*, vol. 15, no. 6, pp. 1–9, Dec. 2021, doi: 10.1007/s11704-021-9460-6.

[6] M. Liu, K. Yang, N. Zhao, Y. Chen, H. Song, and F. Gong, "Intelligent signal classification in industrial distributed wireless sensor networks based industrial Internet of Things," *IEEE Trans. Ind. Informat.*, vol. 17, no. 7, pp. 4946–4956, Jul. 2021, doi: 10.1109/tii.2020.3016958.

[7] C. Lin, G. Han, X. Qi, J. Du, T. Xu, and M. Martinez-Garcia, "Energy-optimal data collection for unmanned aerial vehicle-aided industrial wireless sensor network-based agricultural monitoring system: A clustering compressed sampling approach," *IEEE Trans. Ind. Informat.*, vol. 17, no. 6, pp. 4411–4420, Jun. 2021, doi: 10.1109/tii.2020.3027840.

[8] J. Yick, B. Mukherjee, and D. Ghosal, "Wireless sensor network survey," *Comput. Netw.*, vol. 52, no. 12, pp. 2292–2330, Aug. 2008, doi: 10.1016/j.comnet.2008.04.002.

[9] S. Tomic, M. Beko, and R. Dinis, "3-D target localization in wireless sensor networks using RSS and AoA measurements," *IEEE Trans. Veh. Technol.*, vol. 66, no. 4, pp. 3197–3210, Apr. 2017, doi: 10.1109/TVT.2016.2589923.

[10] T. Çavdar, F. B. Gänay, N. Ebrahimpour, and M. T. Kakáz, "An optimal anchor placement method for localization in large-scale wireless sensor networks," *Intell. Autom. Soft Comput.*, vol. 31, no. 2, pp. 1197–1222, 2022, doi: 10.32604/iasc.2022.020127.

[11] D. K. Sah, K. Cengiz, P. K. Donta, V. N. Inukollu, and T. Amgoth, "EDGF: Empirical dataset generation framework for wireless sensor networks," *Comput. Commun.*, vol. 180, pp. 48–56, Dec. 2021, doi: 10.1016/j.comcom.2021.08.017.

[12] A. Chowdhury and D. De, "Energy-efficient coverage optimization in wireless sensor networks based on Voronoi-Glowworm Swarm Optimization-K-means algorithm," *Ad Hoc Netw.*, vol. 122, Nov. 2021, Art. no. 102660, doi: 10.1016/j.adhoc.2021.102660.
[13] H. Chen, G. Wang, and X. Wu, "Cooperative multiple target nodes localization using TOA in mixed LOS/NLOS environments," *IEEE Sensors J.*, vol. 20, no. 3, pp. 1473–1484, Feb. 2020, doi: 10.1109/JSEN.2019.2948063.
[14] J. Shi, G. Wang, and L. Jin, "Moving source localization using TOA and FOA measurements with imperfect synchronization," *Signal Process.*, vol. 186, Sep. 2021, Art. no. 108113, doi: 10.1016/j.sigpro.2021.108113.
[15] S. Wu, S. Zhang, and D. Huang, "A TOA-based localization algorithm with simultaneous NLOS mitigation and synchronization error elimination," *IEEE Sensors Lett.*, vol. 3, no. 3, Mar. 2019, Art. no. 6000504, doi: 10.1109/LSENS.2019.2897924.
[16] L. Gong, Y. Hu, J. Zhang, and G. Zhao, "Joint TOA and DOA estimation for UWB systems with antenna array via doubled frequency sample points and extended number of clusters," *Math. Problems Eng.*, vol. 2021, Jun. 2021, Art. no. 7521573, doi: 10.1155/2021/7521573.
[17] Y. Wang, S. Ma, and C. L. P. Chen, "TOA-based passive localization in quasi-synchronous networks," *IEEE Commun. Lett.*, vol. 18, no. 4, pp. 592–595, Apr. 2014, doi: 10.1109/lcomm.2014.021214.132662.
[18] G. Wang, W. Zhu, and N. Ansari, "Robust TDOA-based localization for IoT via joint source position and NLOS error estimation," *IEEE Internet Things J.*, vol. 6, no. 5, pp. 8529–8541, Oct. 2019, doi: 10.1109/JIOT.2019.2920081.
[19] Z. Zhou, Y. Rui, X. Cai, and J. Lu, "Constrained total least squares method using TDOA measurements for jointly estimating acoustic emission source and wave velocity," *Measurement*, vol. 182, Sep. 2021, Art. no. 109758, doi: 10.1016/j.measurement.2021.109758.
[20] X. Chen, G. Wang, and K. C. Ho, "Semidefinite relaxation method for unified near-field and far-field localization by AOA," *Signal Process.*, vol. 181, Apr. 2021, Art. no. 107916, doi: 10.1016/j.sigpro.2020.107916.
[21] Y. Wang and K. C. Ho, "An asymptotically efficient estimator in closed-form for 3-D AOA localization using a sensor network," *IEEE Trans. Wireless Commun.*, vol. 14, no. 12, pp. 6524–6535, Dec. 2015, doi: 10.1109/TWC.2015.2456057.
[22] Q. Yan, J. Chen, J. Zhang, and W. Zhang, "Robust AOA-based source localization using outlier sparsity regularization," *Digit. Signal Process.*, vol. 112, May 2021, Art. no. 103006, doi: 10.1016/j.dsp.2021.103006.
[23] T. Zuo, X. Liu, and D. Peng, "UAV path planning for AOA-based source localization with distance-dependent noises," *J. Electr. inf. Technol.*, vol. 43, no. 4, pp. 1192–1198, Apr. 2021, doi: 10.11999/JEIT200078.
[24] S. Xu and K. Doğançay, "Optimal sensor placement for 3-D angle-of-arrival target localization," *IEEE Trans. Aerosp. Electron. Syst.*, vol. 53, no. 3, pp. 1196–1211, Jun. 2017, doi: 10.1109/TAES.2017.2667999.
[25] F. Pang and X. Wen, "A novel closed-form estimator for AOA target localization without prior knowledge of noise variances," *Circuits, Syst., Signal Process.*, vol. 40, no. 7, pp. 3573–3591, Jul. 2021, doi: 10.1007/s00034-020-01624-2.
[26] S. Tomic, M. Beko, and R. Dinis, "RSS-based localization in wireless sensor networks using convex relaxation: Noncooperative and cooperative schemes," *IEEE Trans. Veh. Technol.*, vol. 64, no. 5, pp. 2037–2050, May 2015, doi: 10.1109/TVT.2014.2334397.
[27] G. Wang and K. Yang, "A new approach to sensor node localization using RSS measurements in wireless sensor networks," *IEEE Trans. Wireless Commun.*, vol. 10, no. 5, pp. 1389–1395, May 2011, doi: 10.1109/TWC.2011.031611.101585.
[28] R. Sharma and R. Upadhyay, "Physical layer secure key generation with nonlinear preprocessing of RSS for power constraint wireless networks," *Int. J. Commun. Syst.*, vol. 34, no. 17, Nov. 2021, doi: 10.1002/dac.4985.
[29] R. Zhou, Y. Yang, and P. Chen, "An RSS transform—Based WKNN for indoor positioning," *Sensors*, vol. 21, no. 17, p. 5685, Aug. 2021, doi: 10.3390/s21175685.
[30] J. Qiao, J. Hou, J. Gao, and Y. Wu, "Research on improved localization algorithms RSSI-based in wireless sensor networks," *Meas. Sci. Technol.*, vol. 32, no. 12, Dec. 2021, Art. no. 125113, doi: 10.1088/1361-6501/ac22f1.
[31] X. Guo, N. R. Elikplim, N. Ansari, L. Li, and L. Wang, "Robust WiFi localization by fusing derivative fingerprints of RSS and multiple classifiers," *IEEE Trans. Ind. Informat.*, vol. 16, no. 5, pp. 3177–3186, May 2020, doi: 10.1109/TII.2019.2910664.
[32] B. Wang, X. Gan, X. Liu, B. Yu, R. Jia, L. Huang, and H. Jia, "A novel weighted KNN algorithm based on RSS similarity and position distance for Wi-Fi fingerprint positioning," *IEEE Access*, vol. 8, pp. 30591–30602, 2020, doi: 10.1109/ACCESS.2020.2973212.
[33] P. Zuo, T. Peng, H. Wu, K. You, H. Jing, W. Guo, and W. Wang, "Directional source localization based on RSS-AOA combined measurements," *China Commun.*, vol. 17, no. 11, pp. 181–193, Nov. 2020, doi: 10.23919/jcc.2020.11.015.
[34] M. S. Costa, S. Tomic, and M. Beko, "An SOCP estimator for hybrid RSS and AOA target localization in sensor networks," *Sensors*, vol. 21, no. 5, p. 1731, Mar. 2021, doi: 10.3390/s21051731.
[35] S. Kang, T. Kim, and W. Chung, "Multi-target localization based on unidentified multiple RSS/AOA measurements in wireless sensor networks," *Sensors*, vol. 21, no. 13, p. 4455, Jun. 2021, doi: 10.3390/s21134455.
[36] S. Tomic, M. Beko, L. M. Camarinha-Matos, and L. B. Oliveira, "Distributed localization with complemented RSS and AOA measurements: Theory and methods," *Appl. Sci.*, vol. 10, no. 1, p. 272, Dec. 2019, doi: 10.3390/app10010272.
[37] S. Boyd and L. Vandenberghe, *Convex Optimization*. Cambridge, U.K.: Cambridge Univ. Press, 2004.
[38] S. Chang, Y. Zheng, P. An, J. Bao, and J. Li, "3-D RSS-AOA based target localization method in wireless sensor networks using convex relaxation," *IEEE Access*, vol. 8, pp. 106901–106909 2020, doi: 10.1109/ACCESS.2020.3000793.
[39] S. Tomic, M. Beko, R. Dinis, and L. Bernardo, "On target localization using combined RSS and AoA measurements," *Sensors*, vol. 18, no. 4, p. 1266, Apr. 2018, doi: 10.3390/s18041266.
[40] S. Tomic, M. Beko, and R. Dinis, "A closed-form solution for RSS/AoA target localization by spherical coordinates conversion," *IEEE Wireless Commun. Lett.*, vol. 5, no. 6, pp. 680–683, Dec. 2016, doi: 10.1109/LWC.2016.2615614.
[41] S. Kang, T. Kim, and W. Chung, "Hybrid RSS/AOA localization using approximated weighted least square in wireless sensor networks," *Sensors*, vol. 20, no. 4, p. 1159, Feb. 2020, doi: 10.3390/s20041159.
[42] F. Watanabe, "Wireless sensor network localization using AoA measurements with two-step error variance-weighted least squares," *IEEE Access*, vol. 9, pp. 10820–10828, 2021, doi: 10.1109/ACCESS.2021.3050309.

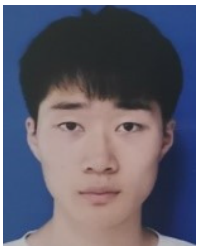

WEIZHONG DING entered the Ningbo University of Technology, China, in 2018. His current research interests include wireless localization and underwater acoustic wireless sensor networks localization.

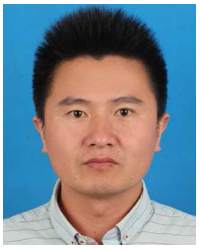

SHENGMING CHANG received the B.Sc. degree in mathematics from the Leshan Teachers College, Leshan, China, in 2008, the M.Sc. degree in applied mathematics from Ningbo University, Ningbo, China, in 2014, and the Ph.D. degree from the Faculty of Electrical Engineering and Computer Science, Ningbo University, in 2019. He is currently a Lecturer of electronic engineering with the Ningbo University of Technology, Ningbo. His current research interests include wireless localization and underwater acoustic wireless sensor networks localization.

JUN LI received the B.Sc. degree in computer science and technology from Jiamusi University, Heilongjiang, China, in 2003, the M.Sc. degree in computer application technology from Xihua University, Chengdu, China, in 2008, and the Ph.D. degree in computer application technology from Shanghai University, China, in 2011. She is currently a Lecturer of electronic engineering with the Ningbo University of Technology, Ningbo, China. Her research interests include virtual reality, machine learning, and multimedia information processing.